GAWAC 3.0

Gabion wall design

GSC Manual

Petrucio Santos Junior

Nicola Mazzon

Ratnakar R. Mahajan

Paolo Di Pietro

Version 1.0

April 2019

MACCAFERRI

Summary

1. Introduction

The use of double twisted mesh gabions is a well-established technical solution for the construction of retaining structures. Following the evolution of the more general framework of the civil engineering approaches, the design of retaining structures has been generally refined over the last decades to improve their overall safety. Within this evolution, the most advanced design methodologies in the field of the civil engineering are performance-based, depending both on the materials employed and on the actions. Furthermore, several additional aspects influencing the overall behavior of the structures shall be considered to guarantee an adequate safety level. Indeed, the designers are then nowadays required to verify the performance of a structure not only against the failure, intended as the achievement of the maximum strength of the materials. Further requirements shall be satisfied such as the behavior under service- or fatigue conditions. Furthermore, the concept of "working life" of a structure has been introduced since long time with the aim of guaranteeing the design requirements to be satisfied over the time and until the end of the estimated life.

Nevertheless, a lack of knowledge on the overall behavior of gabion structures shall be highlighted on these bases. As a consequence, this directly reflects on a higher design uncertainty and then in an overall lower safety condition. The current design approaches of gabion retaining structures consider only some of the above-mentioned aspects. Among the most relevant, both the overall behavior under service conditions and the change in the mechanical performances of the materials over the time are usually neglected.

The historical and wide experience of Officine Maccaferri in the field of double torsion, especially on double twisted mesh gabions joined with the aim of a continuous innovation have been leading to develop a research project both to tackle the above highlighted issues and to cover the gaps between current practice and normative requirements. In this light, a wide research project was jointly developed by Officine Maccaferri Spa through its subsidiaries Officine Maccaferri do Brasil and Maccaferri Innovation Center. As a result, this study thus allows to move further steps ahead in the knowledge of the gabion retaining structures and on the performance of the double twisted steel mesh.

The main outcomes are the definition of a novel mechanical parameter characteristic of the double twisted steel mesh and a performance-based approach suitable to control the behavior under both service- and long term-conditions. This new parameter is named as Gabion Serviceability Coefficient (GSC). The whole research program involved a wide experimental campaign that allowed the subsequent development and calibration of detailed numerical models. Based on the results of both investigations, an analytical approach is then developed to evaluate the safety of a gabion retaining structure through a Safety Factor. A comprehensive overview of the whole research is presented on this document together with the new proposed design approach.

2. Gabion retaining structures

Gabions are steel wire mesh containers of variable sizes, uniformly partitioned into internal cells, interconnected with other similar units, and filled with stone at the project site to form permeable, monolithic structures such as retaining walls, channel linings, revetments and weirs for erosion control projects (definition from ASTM A975).

The gabion is considered a structured element. The metallic mesh provides a lateral restrain to the filling material, thus allowing the achievement of the gabion metallic properties. The same mechanical behavior cannot be guaranteed by loose stones. Furthermore, the presence of the steel mesh allows both the out-of-plane displacements to be controlled and, consequently, the load capacity of the gabion element to be increased. When installed, the gabions form a monolithic structure suitable for different applications. Indeed, the mechanical characteristics of the gabion allow to create a structural element resistant to both internal compressive and tensile stresses.

Since the metallic mesh is responsible for the mechanical behavior of the gabions, studying its mechanical properties, becomes a determining task in the attribution of the hypotheses that establish the mathematical concepts used in the calculation methods used.

The box gabion is typical in retaining walls and is the basis of this study. It is an element produced to form cells of volume of one or half cubic meter, through the application of diaphragm panels to each meter (Figure 1).

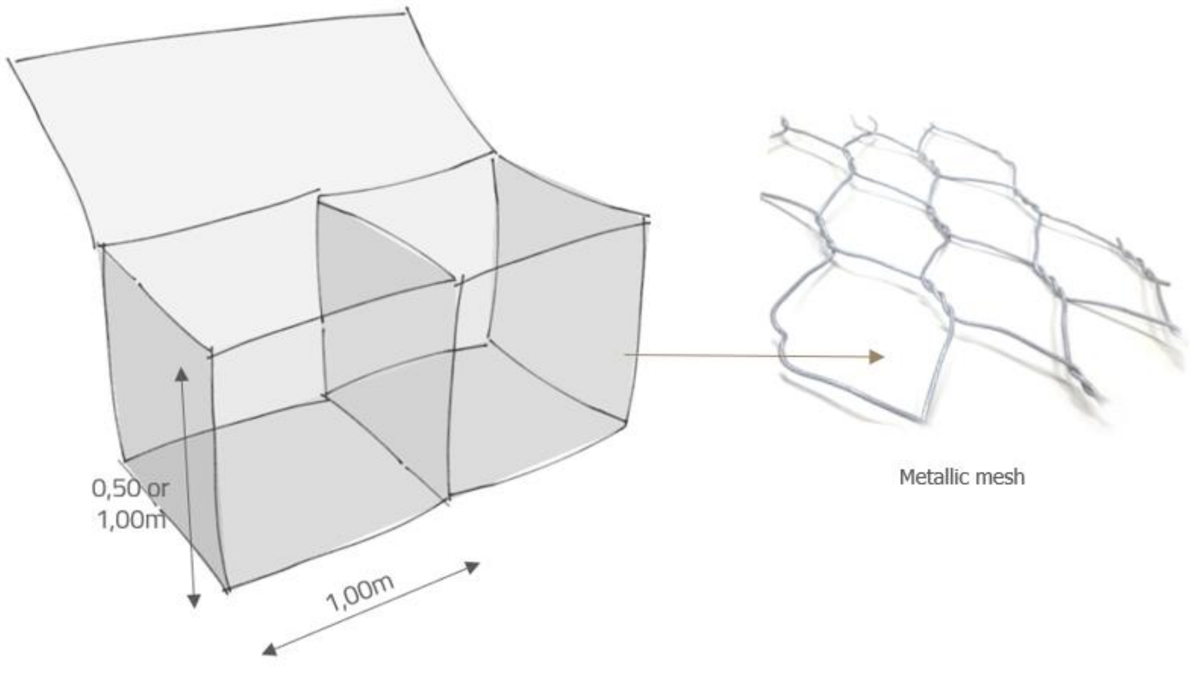

Figure 1 – Example of box gabion 2.0m x 1.0m x 1.0m, with diaphragms each meter.

The gabions are arranged in horizontal layers in the retaining walls and they have a lateral restriction provided by the adjacent gabions.

Thus, the front face of a retaining wall in a gabion is free to displace according both to the mechanical properties of the metallic mesh and to the normal pressure caused by the filling material and soil retained, being these the relevant components considered in the structural verifications of a wall.

The structural design of retaining walls considers that the gabions are installed in layers and each of them acts as a unitary structural element. The monolithic overall behavior of the wall is guaranteed by the lacing wires installed on the edges of the gabions and linking contiguous gabions.

In practice it is known that gabions are subjected to long-term loading and a detailed study of such behavior may help the designer to determine whether a deformation is caused by service condition or construction error. Gabions are divided into cells of one meter wide and for this reason a single gabion element is taken as a reference and its behavior must be analyzed when subjected to a certain level of pressure (Figure 2). This approach will be considered in this report and the results of this study will be applied as a theoretical basis for the development of stability analyzes.

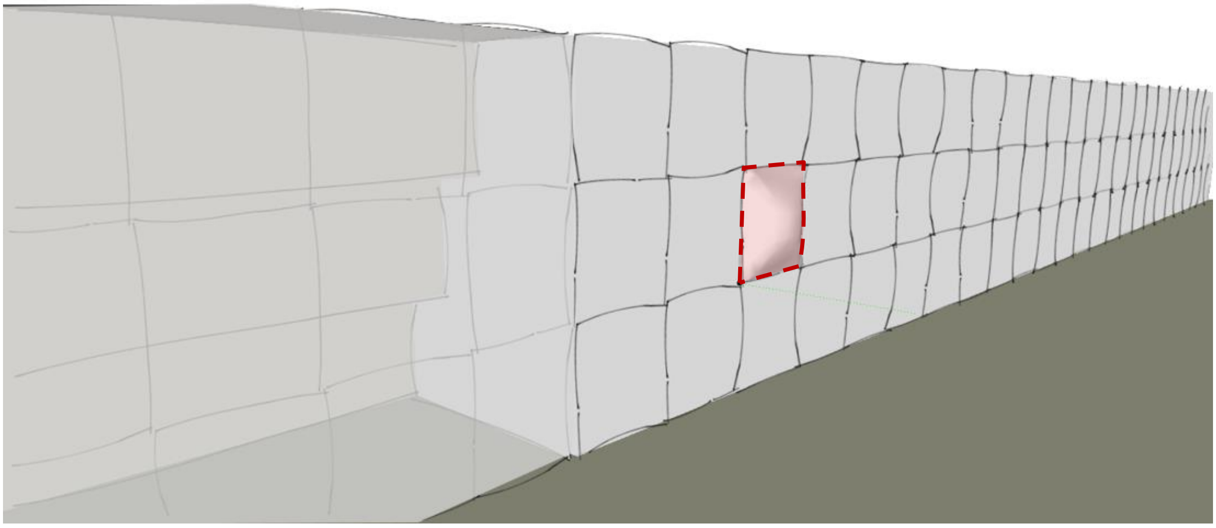

Figure 2 – Single gabion element within a gabion retaining structure.

3. Early studies on gabions

In order to achieve a comprehensive knowledge about the behavior of gabion structures, Agostini et al. (1987) carried out a wide experimental campaign.

- In the first phase, compression tests were performed on gabion elements and on the metallic mesh that composes these elements to determine deformability and tensile strength parameters;
- In the second phase, load tests were performed on real-sized retaining walls (height of 4.0 m) to evaluate the results obtained in the first phase and the eventual determination of limit values;
- In the third phase, pullout tests were carried out on hexagonal mesh panels confined to various soil types in order to determine the ability of such panels as reinforcing elements in reinforced soil structure.

The third phase will not be commented in this work, because it is an experiment carried out with the purpose of knowing the behavior of the metallic mesh in confined conditions, for soil reinforcement purposes.

3.1. Compression test in gabions

The compression tests were carried out at the *Laboratorio di Scienza delle Costruzioni* at the University of Bologna in 1979, using specimens consisting of one or more gabions (connected to each other) of nominal dimensions 0.50m x 0.50m x 0.50m and double-twist hexagonal mesh, with hexagons of dimensions 6 cm x 8 cm and wire diameter of 2.7 mm, tied by wire of 2.4 mm diameter and filled manually by stones. Figure 3 shows the compression test, without lateral restrictions, with vertical load applied on the gabion element to provide an indication of its maximum compressive strength.

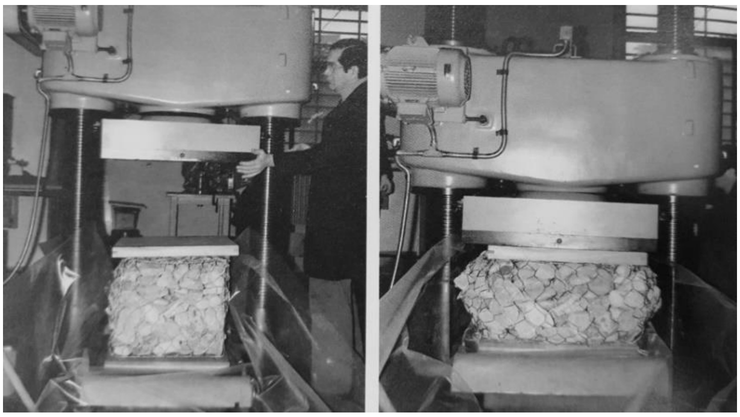

Figure 3 - Compression test in gabions (AGOSTINI et al., 1981).

3.2. Compression test with lateral restraint

Agostini et al. (1987) give a brief account of the lateral restriction tests. These tests were executed on samples similar to those tested in the compression test confined on opposite sides by two rigid metal plates in order to restrict lateral displacements.

The plates were lubricated to reduce the friction between them and the gabion. These tests were conducted in the same way as the simple compression tests and were finalized when the plates became very distorted or when the unconfined faces touched the guide bars of the press.

According to Agostini et al. (1987), the overall result did not differ substantially from the unrestricted tests, showing also an initial adjustment of the stones and internal rupture of the inner core. It was not possible, even at high loads, to bring the gabion mesh.

Figure 4 represents the average behavior of the samples tested with and without lateral restriction, in which higher stiffness is observed in the restriction tests.

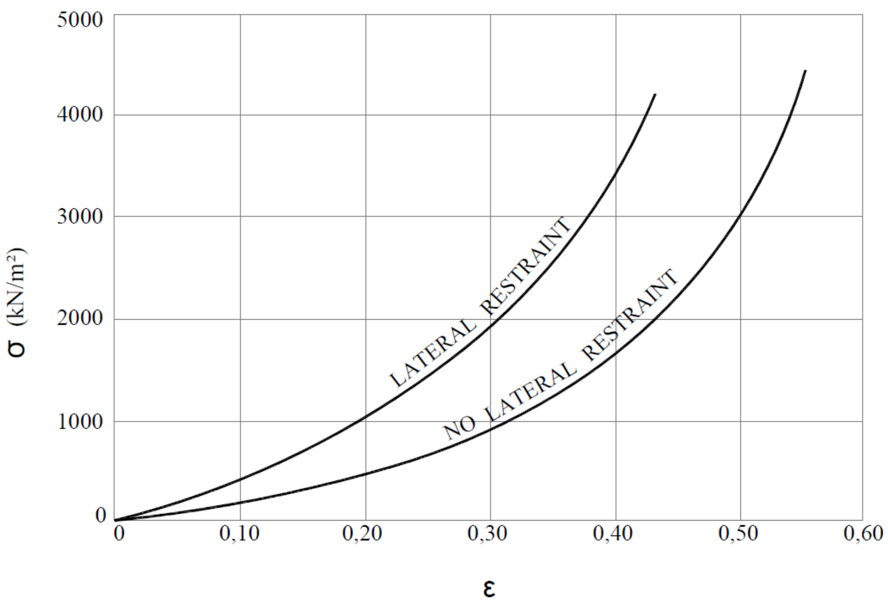

Figure 4 - Results of compression tests in gabions, with and without lateral restriction (AGOSTINI et al., 1987).

4. Mechanical properties of gabion components

Over the years the gabions have changed mainly in the metallic mesh that compose them. The mechanical properties of these meshes have characteristics that have been improved and such properties must be evaluated to understand the behavior of the gabion elements.

The double-twist hexagonal mesh composing the gabion is a traction resistant element, manufactured from steel wire entanglement of the double-twist steel wire forming hexagons of the same size.

The characteristic dimension of the hexagons refers to the distance “D” between two parallel twists of the same mesh, measured from the inside of one twist to the outside of the other (Figure 5).

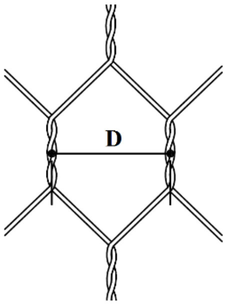

Figure 5 - Mesh dimension.

4.1. Properties of wires used in gabion mesh

The wires used in the fabrication of the double-twist hexagonal mesh are composed of an iron and carbon alloy, generally containing less than 0.1% carbon, in addition to other alloying elements, i.e. with low carbon and low alloy content. It is a ductile steel, soft, easily folding and conforming in stamping.

These wires pass through a production process that starts from the raw material and follows through phases of drawing, galvanizing and optional plastic coating by extrusion.

The raw material is supplied in rolls of 1,500 to 2,000 kg with a nominal diameter of 5.5 mm (+/- 3%) and presents an appropriate chemical composition. The strength of the wire used for the production of the double twisted mesh shall range between 350 MPa and 550 MPa and the elongation shall be higher than 10%.

The wires used in the fabrication of gabion mesh are evaluated by the tensile test. This test results in a graph presenting a material of ductile behavior, i.e. it can be elongated, flexed or twisted, without breaking. Figure 6 shows a typical stress-strain trend of a single wire, where δw is the axial strain, δw_{max} is the maximum axial strain, Fw is the axial tensile stress of wire and Fw_{max} is the maximum axial tensile stress of wire.

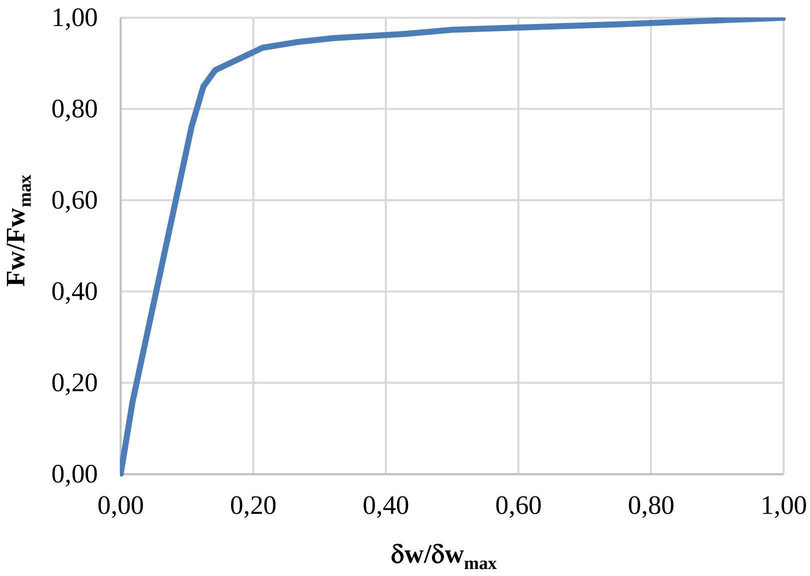

Figure 6 - Results of a typical tensile test for steel wire.

4.2. Properties of the mesh

The procedures for tensile testing of the double-twist hexagonal mesh follow the guidance of EN 10223-3: 2013 "Steel wire and wire products for fencing and netting".

Based on this test it is possible to obtain the value of tensile strength per meter of mesh in the direction parallel to the twisting (Figure 7).

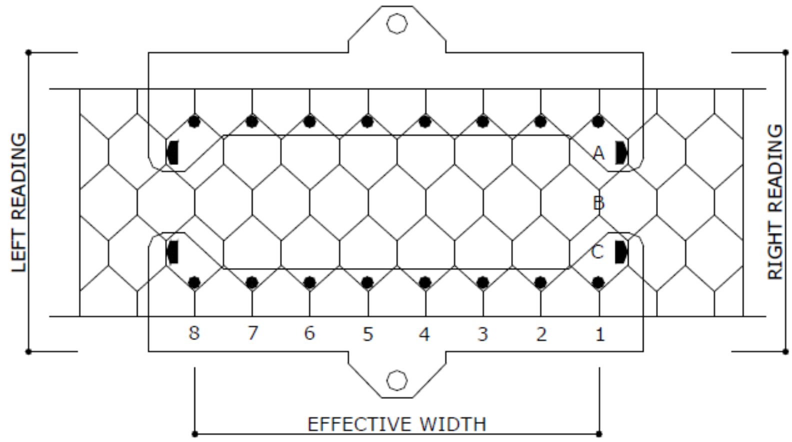

Figure 7 - Schematic of the tensile test according to EN 10223-3: 2013.

The results of the tensile tests performed on the hexagonal mesh of the gabion element reveal proportionality between the tensile strain and the deformation of the mesh and for this reason the characterization graphs of this material refer to elastic-linear behavior.

Currently, there are several standards that define the mechanical and durability properties of gabion metal meshes. Appendix B lists the main international standards that refer to double-twist hexagonal mesh.

Although the tensile test is commonly used to characterize the mechanical properties of the gabion metal mesh, other tests can provide relevant mechanical parameters suitable to describe its mechanical behavior. This is the case of the punching test.

The punching test is performed by fixing a specimen of double-twist hexagonal mesh to a steel frame with nominal dimensions of 1,0 m x 1,0 m (Figure 8). The punching effect is achieved through a 350mm diameter steel dome placed between the hydraulic jack and the specimen.

The load is applied perpendicularly at the center of the specimen at a constant velocity of 10 mm / min. The test ends when the first wire breaks (Figure 8).

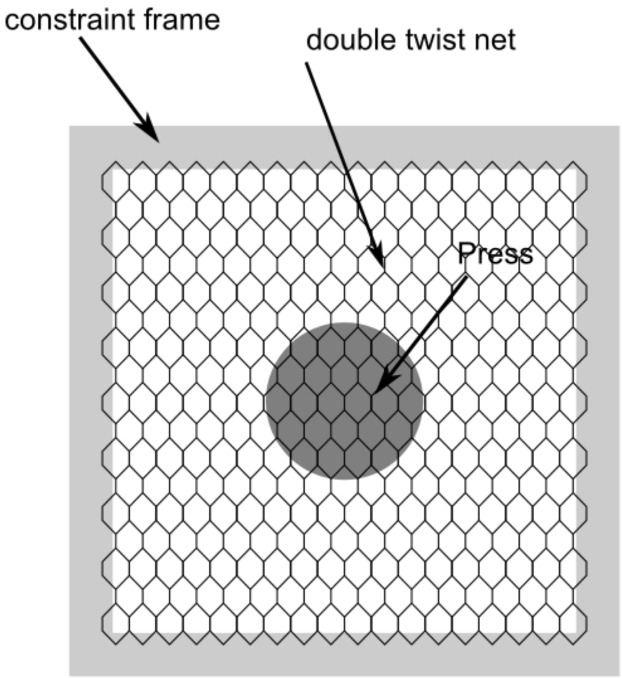

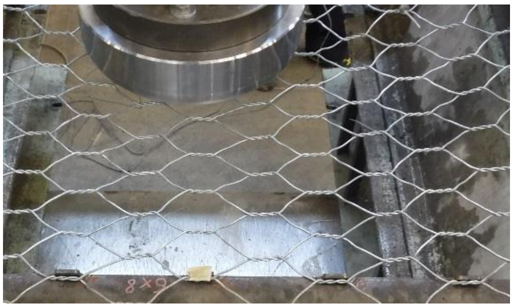

b)

a)

c)

Figure 8 – Punching test: a) Detail of the sample placed on the steel frame; b) fixing the mesh to testing; c) sample in the moment of rupture.

4.3. Characteristics of the filling material

Stone elements are commonly used to fill the gabions. This material must be composed of particles of various sizes and angularity, allowing grouping and interconnection. The dimensions of the particulate elements used in the filling should range from one to two and a half times the mesh opening, namely the distance between the twisting stretches of the mesh. Dimensions outside these limits will only be allowed when justified and specified in design. Furthermore, it must be a durable material of suitable mineralogy, free of adhesive dust or deteriorating material, in addition to including few flat or elongated particles.

The mechanical behavior of the gabions depends on the quality of the filling material and on the contact interlocking between stones.

The point-to-point contact of the surfaces of the filler elements must be maintained and anything that affects this interaction can cause problems in the gabion behavior (Figure 9).

Figure 9 – Point-to-point contact causing load transfer at these points.

5. Hypotheses and prediction of the results

The currently adopted design codes usually requires carrying out verifications not only under ultimate conditions but also under service conditions. This can be achieved only through an in-depth knowledge of the mechanical behavior of both single gabion and whole gabion retaining structure.

Figure 10 presents a simplified scheme of the internal forces acting on each layer of gabions. Figure 10a shows the vertical pressure acting on each gabion layer by assuming that the normal force distributes uniformly along the exposed face to the edge of the gabion layer.

This vertical pressure causes horizontal pressure. Considering that only the front part of each gabion layer is not confined and therefore free to move, the horizontal pressure is assumed to be sustained by the metallic mesh that acts as a confinement of the filling material.

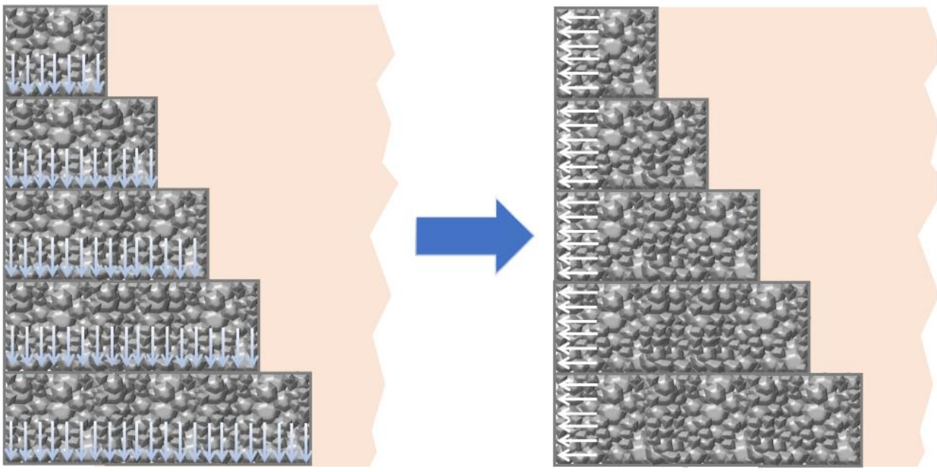

a) b)

Figure 10 – Pressures acting on the layers of a gabion wall: a) Vertical pressure per layer; b) induced horizontal pressure applied on the external face of the wall by layer.

Figure 11 shows as the behavior of the front face of the gabion, which under load condition, acts as an elastic membrane. The horizontal pressure causes a deflection in the metallic panel confining the fill material resulting from stress transfer and the balance of forces present in the internal stability of each stratum composing the retaining wall.

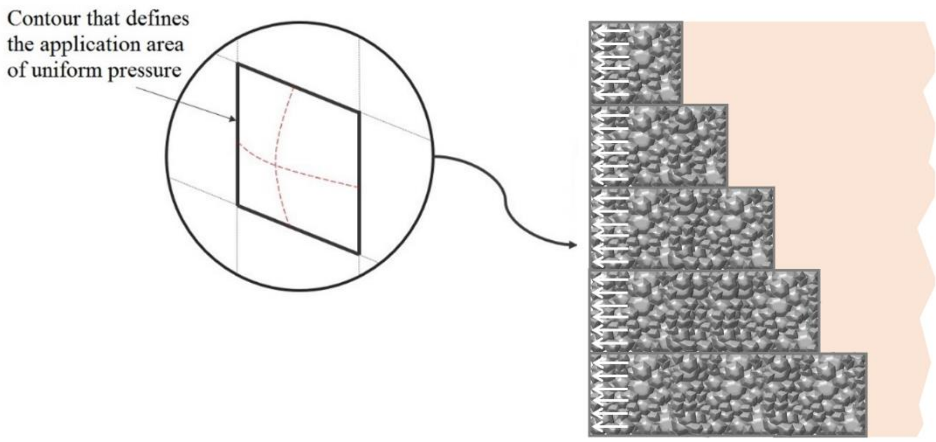

Figure 11 - Contour that defines the metallic panel under pressure.

This behavior can be seen through observations in several works over several years of experience in monitoring the installation process and service conditions and in the fact that the hexagonal mesh has an elastic-linear behavior. The metallic mesh can be assumed to behave as an elastic membrane since its thickness is very reduced in relation to the low level of deflection caused by the working pressure.

The subsequent chapters demonstrate through experimental, numerical and analytical studies that this approach is suitable to provide a calculation method for the analysis of the internal stability of gabion retaining walls. This can be then exploited to carry out analyses under service conditions, thus answering the normative requirements and then the needs of the designers.

5.1. Experimental investigation

A new wide experimental campaign was carried out in three laboratories from different countries to complete the lack of knowledge highlighted on the previous section also to answer to the mentioned normative requests. More than 30 compression tests were performed and different positions for the instruments were proposed before reaching the results presented here. The final results of these experimental compression tests are hereafter summarized. The analysis of the tests allowed to determine more precise results as the tests were done.

Gabion compression tests were carried out in three different laboratories:

- Experimental Institute for Geotechnical Modelling (ISMGEO), Bergamo, Italy.
- Structural Engineering Laboratory of State University of Campinas (UNICAMP), Campinas, Brazil;
- Geotechnical Engineering Laboratory of Department of Civil Engineering, Indian Institute of Technology (IIT), Roorkee, India;

The first tests were carried out in Brazil on samples of gabions in real size. Subsequently, new test campaigns were conducted both in India and in Italy. In addition to locally produced gabions, rocks with different geological characteristics were used. It was attempted to standardize the tests so that the analysis of the results could provide similar parameters.

The gabions were stored on wooden pallets (Figure 12), so it was possible to handle samples with mechanized equipment inside the laboratory space. Figure 12 shows the gabions stored inside the laboratory. Figure 13 shows the transport of the gabion sample with forklift and the lifting of the samples for later positioning under the hydraulic jack.

The gabions were installed on a 10 mm thick rubber plate placed on a steel base (Figure 14). Bracing wires with 2.20 mm were placed symmetrically, that is, fixed from one side to the other in both directions, respecting the standard positioning for height (Figure 14).

a) b)

Figure 12 - Assembly of gabions: a) pre-assembled gabions; b) gabions stored inside the laboratory.

a) b)

Figure 13 - Handling of the gabion sample: a) gabion transport with fork-lift; b) lifting and placing on site of the jack.

a)

b)

Figure 14 - Installation details: a) rubber pad and metal plate placed under the gabion element; b) wire rods in both directions.

Confined and unconfined compression tests were performed following similar load application patterns, differing mainly by the results that were obtained due to the different positioning of the measuring instruments. The following will present the results and a brief discussion on the performance of the compression tests.

Table 1 presents the results obtained in the compression tests performed under the restricted and unrestricted condition.

According to the results presented in Table 1, the maximum recorded vertical pressure value of the restricted condition is approximately 3 (three) times that of the unrestricted condition and the ratio between the maximum vertical pressure of the gabion box with 0.50 m high is approximately 1.50 times greater than the box value with 1.00 m high.

Table 1. Maximum vertical pressure for gabions under restricted and unrestricted condition.

Restricted condition	
	Vertical pressure (kPa)
10x12, 2,7mm – 1,00m	900
8x10, 2,7mm – 1,00m	950
10x12, 2,7mm – 0,50m	1350
8x10, 2,7mm – 0,50m	1400
Unrestricted condition	
	Vertical pressure (kPa)
10x12, 2,7mm – 1,00m	300
8x10, 2,7mm – 1,00m	300
10x12, 2,7mm – 0,50m	400
8x10, 2,7mm – 0,50m	450

Direct shear tests were also executed with and without the gabion mesh to evaluate the contribution given by gabion and stones, respectively on the overall results. Two horizontal and four vertical transducers were installed to measure the horizontal and vertical deformations.

The tests were conducted under different normal stresses as 80 kPa, 100 kPa, 150 kPa and 200 kPa for both gabion shear and stone shear testing. Experiments were carried out at constant strain rate of 0.4 mm/min up to 10% of the specimen length i.e. 75 mm. From the points measured in the tests it is possible to draw a simple linear regression curve and determine a value of internal friction angle and an intercept value for both studied cases.

The difference between the angular coefficients of both straight lines is small, but the difference between the linear coefficients is high (Figure 15), where σ is the normal stress, σ_{max} is the maximum normal stress, T is the shear stress and T_{max} is the maximum shear stress. This is due to the interference offered by the small dimensions of the box, thus a scale factor has to be considered. As the shear box has a lower cross section than the standard dimensions of a conventional gabion (0.75 m x 0.75 m), a scale correction factor was proposed for the determination of the cohesive intercept.

According to Dell'avanzi et al. (2006) the geometric scale factor between prototype and model, *N*, defines the relationship between the lengths of the prototype and model. Mathematically, *N* is defined by:

$$N = \frac{L_p}{L_m} \qquad (1)$$

where L_p is the length of the prototype, and L_m is the length of the model. Equation 1 indicates that the length of the model should always be N times less than the length of the prototype.

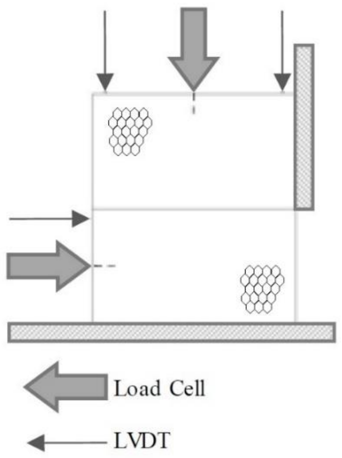

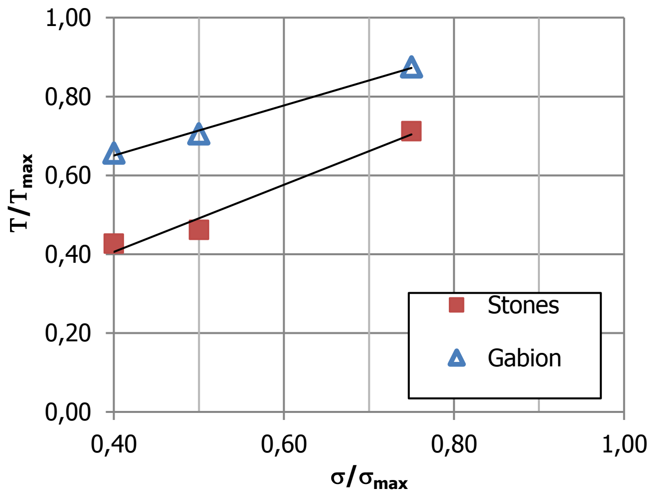

a) b)

Figure 15. Direct shear test; a) position of instruments; b) shear stress vs normal stress plot of gabion shear.

Table 2 shows a relation of scale factors to be observed in models tested in terrestrial gravity to guarantee similitude of behavior between model and prototype.

Table 2. Scale Factors (Dell'avanzi et al., 2006)

Greatness	Scale factor (prototype / model)
Acceleration	1
Length	N
Area	N^2
Volume	N^3
Force	N^3
Density	1
Mass	N^3
Specific weight	1
Tension	N
Friction angle	1
Porosity	1
Elasticity Module	N
Cohesive Intercept	N

Considering that $N = 0.70$, there is a factor that allows to correct the shear stress value applied along the shear plane (Figure 16) and it can consider the total shear stress for the gabion is represented by:

$$S_g = S_s + S_{ms} \tag{2}$$

where S_{ms} is the shear stress of the mesh in scale and S_s is the shear stress of the stones.

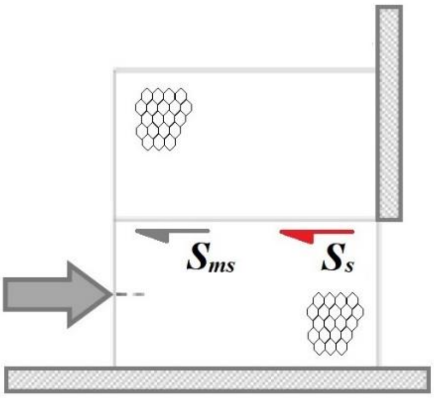

Figure 16. Shear stresses acting on the shear plane of the gabion specimen.

Equation 3 demonstrates the adjusted shear stress for the gabion considering the scale factor.

$$S_{gc} = S_g N^2 \tag{3}$$

According to Figure 18 the value of the intercept of the gabion with 10x12 mesh is 202,25 kPa. Using the Equation 3 to correct this value considering the appropriate scale factor is possible to get the equivalent intercept of the gabion as equal to 99,10 kPa.

The value of the internal friction angle is not influenced by the scale and its value can be adopted as being equal to 54 degrees. Table 3 shows the computed mechanical parameters for the tested meshes, considering a reduction factor of 1.3 for the intercept. These values refer to the effective cohesion of the gabion element.

Table 3. Gabion resistance parameters.

Mesh	Friction angle (degrees)	Intercept (kPa)
8x10, 2,7mm – 1,00m	54	93
10x12, 2,7mm – 1,00m	54	76

Agostini et al. (1987) studied apparent cohesion concerning the connection between gabion elements. These values depend on the ratio of weight of mesh to the volume of the gabion structure, and it increases as the gabion depth decreases, with gabions filled with diaphragms, and with gabions constructed of heavier mesh.

Conversely the value of adhesion decreases with the increase in gabion thickness, with gabions without diaphragms, with large mattress type gabions, and with gabions made of lighter mesh. It is possible to compute the representative apparent cohesion using the empirical expression,

$$c_g = 0{,}3P_u - 0{,}5 \tag{4}$$

where P_u is the weight of the metallic mesh per cubic meter of wall expressed in kg/m³ and c_g is expressed in tf/m².

The value of the gabion/stone filling friction angle depends upon different factors: the stone/rocks angularity (φ increase with the angularity), the granulometry (φ increase with the grain non-uniformity) and the density (φ increases with the density).

From the apparent cohesion and friction angle values between gabions it is possible to determine the allowable shear stress,

$$\tau_{adm} = N \tan\varphi + c_g \tag{5}$$

where N is the normal force on the respective layer.

The results obtained through the new experimental investigation are considered more accurate than the results obtained through the formulation presented in equations 4 and 5 and for this reason be used as a reference from now.

5.2. Numerical analyses

A wide numerical study has been developed to better understand the mechanical behavior of both double twisted mesh and gabion element. This allows to investigate the stress-strain behavior under different loading conditions, representing the first step for a subsequent analytical description of the mechanical behavior of both gabion element and gabion structure.

Based on the numerical study initiated by Thoeni et al. (2011), which simulates the double-torsion hexagonal mesh behavior with the discrete element method (DEM). This new model is calibrated according to the results of the punching tests based on mesh panels measuring of 1.00 m x 1.00 m. This size approximates the dimensions of the outer vertical face of a gabion. Figure 17 shows the result of a simulation.

Figure 18 compares the experimental results of punch tests for a standard mesh panel 8x10, 2.7 mm, where Fp is the punching force. Fp_{max} is the maximum punching force, δp is the displacement and δp_{max} is the maximum displacement. double-twist hexagonal mesh panels with the results obtained through a DEM model. Since the numerical results are similar to the experimental results is possible to create a standard average behavior to be calibrated for this specific mesh typology and also reproduce the same model for other types of mesh once respecting the same mechanical properties of the wire used.

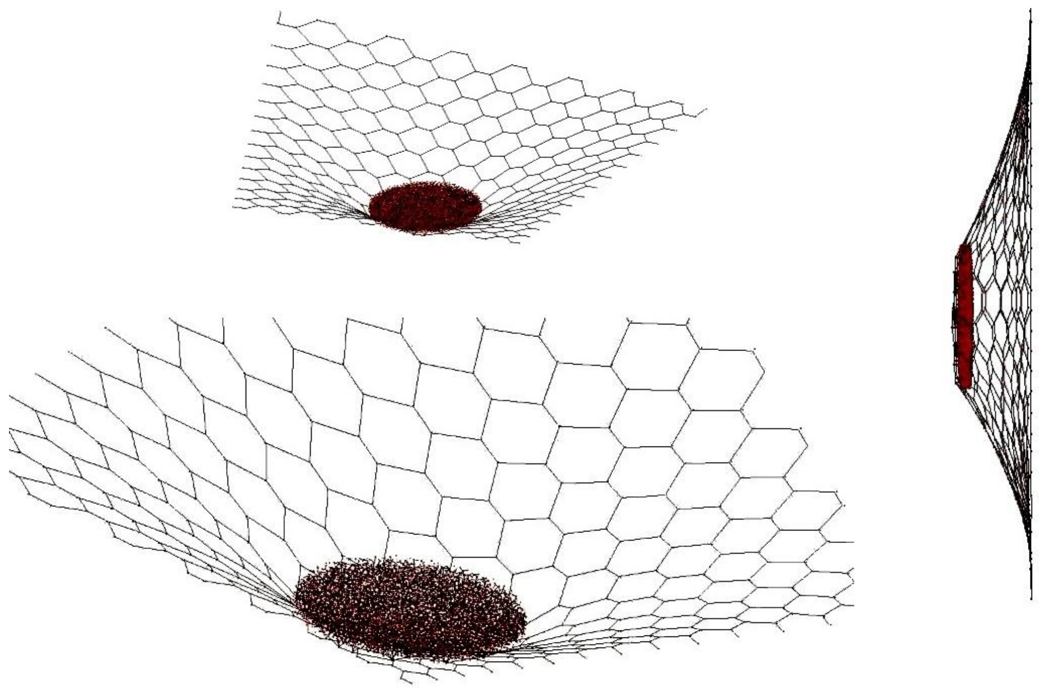

Figure 17 - Numerical simulation of the punching test of the hexagonal mesh (SANTOS JUNIOR, 2018).

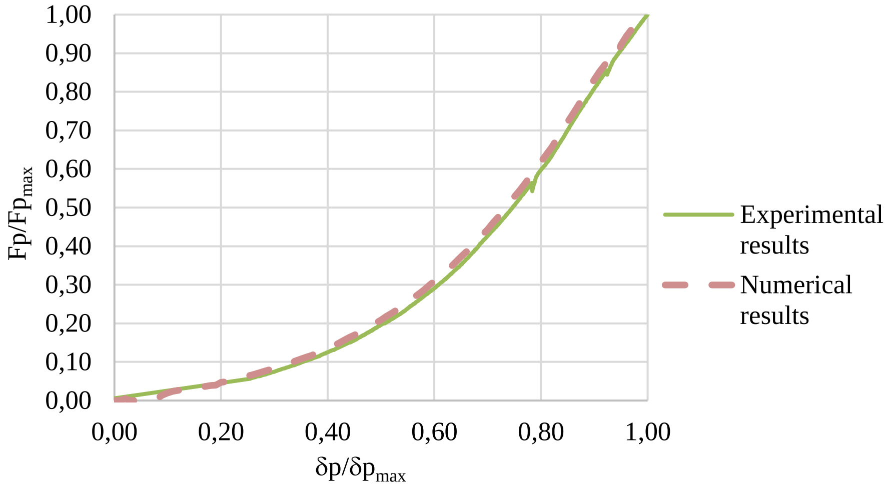

Figure 18 – Normalized comparison between numerical and experimental results for punching in hexagonal mesh.

The second phase of the numerical investigation is the development of a model suitable to reproduce the overall behavior of a whole gabion.

Then, after calibrating the numerical model for the metallic mesh the calibration of the gabion filled with particulate materials was simulated. As a first approach, a numerical model of the gabion cage was randomly filled by polyhedral elements. Figure 19 shows a comparison between numerical and experimental results, where Vp_{max} and Vd_{max} are the maximum pressure and vertical displacement obtained in the regular test, respectively.

Simulations were performed using polyhedrons and sphere clumps were used and both results were similar (Figure 19 and 20). Due to the computational simplicity, it was decided to use sphere clumps. Indeed, the model using spheres is computationally faster and presents results as good as the previous one (Figure 20).

Restricted compression tests were also performed and therefore, a numerical model was also created to simulate the same experimental conditions (Figure 21).

After calibrating the numerical model of the gabion element, it was possible to study its behavior under several technical aspects. One of the most relevant aspect to be deeply investigated is the relation between vertical and horizontal pressure. Since this relationship allows a simpler analytical approach to be developed.

Furthermore, the analysis of both vertical and horizontal acting pressures allows also the analysis of the outer unconfined side of the gabion, that represents the front face of the retaining wall. From several numerical analyses the following ratio between horizontal and vertical pressure has been found:

$$\frac{\text{horizontal pressure}}{\text{vertical pressure}} \approx 0{,}10 \tag{6}$$

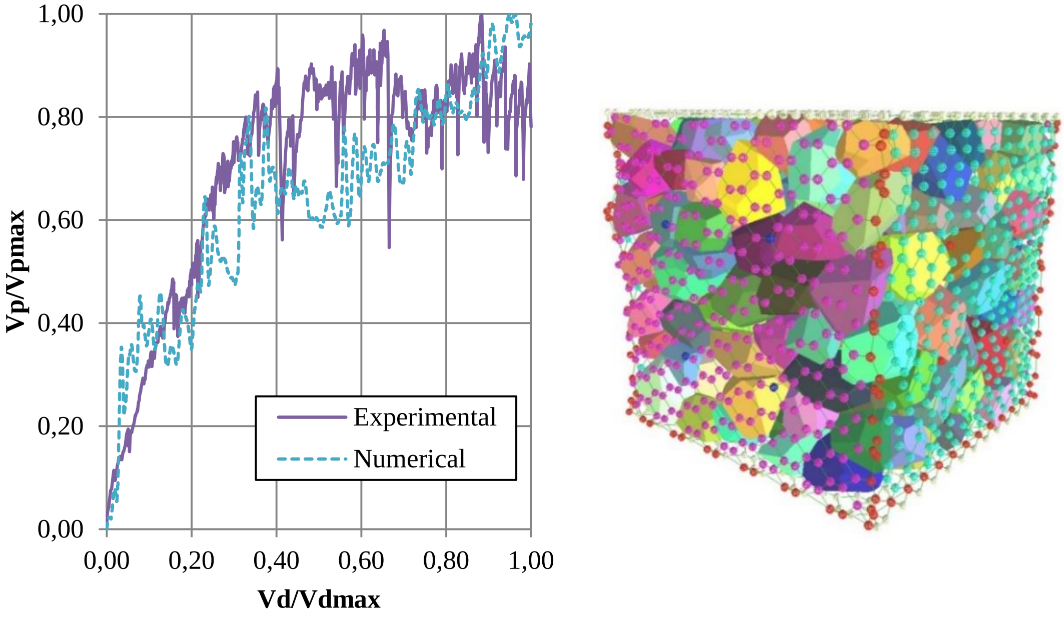

a) b)

Figure 19 – Model in DEM of a gabion filled with polyhedra; a) comparing the results in DEM using polyhedra with the experimental results; b) 3D view of a gabion in DEM filled with polyhedral (SANTOS JUNIOR, 2018).

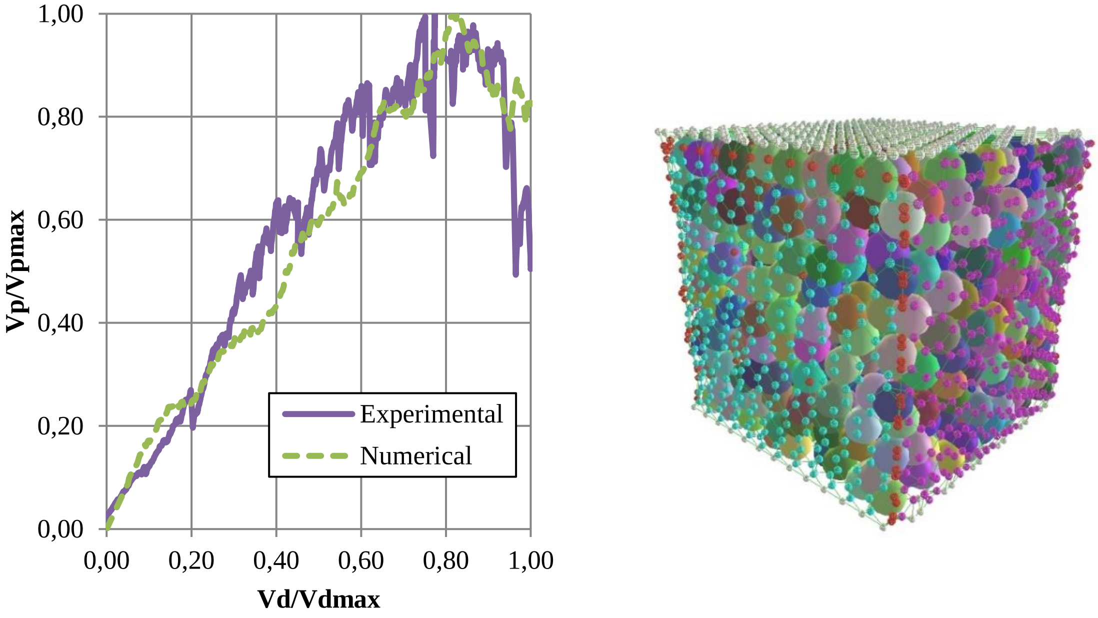

a) b)

Figure 20 – Model in DEM of a gabion filled with spheres; a) comparing the results in DEM using spheres with the experimental results; b) 3D view of a gabion in DEM filled with spheres (SANTOS JUNIOR, 2018).

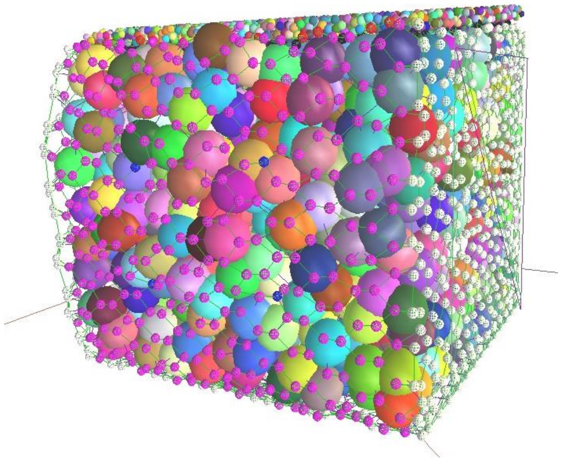

a) b)

Figure 21 - Rotation of the load application plate on the restricted gabion sample: a) experimental model; b) numerical model (SANTOS JUNIOR, 2018).

In the initial loading condition, in which the gabion mesh is about to be loaded, it is possible to say that the relation between the horizontal and vertical pressure equals the active thrust coefficient, k_a.

Considering the value of k_a = 0.1 (Table 3), it is possible to calculate the equivalent internal friction angle, ϕ, between the particles, $\phi \approx 54º$. This result is compatible with the experimental and numerical results obtained and can be used as reference value for the gabions, once the installation process is accepted.

5.3. Elastic membrane

It is observed that the mesh of the gabion when subjected to a uniform pressure has a behavior very close to that of an elastic membrane. Thus, one of the hypotheses that can be used in the simplified calculation model is that the hexagonal mesh is considered as an elastic membrane of very thin thickness, flat and subject to a uniform tensile force, T, when deformed.

When fixing this membrane along a contour, a uniform pressure p is applied in the direction perpendicular to the membrane surface. This membrane deforms, assuming the shape of a curved surface, Figure 22, which can be described by the two-dimensional Poisson equation.

$$\frac{\partial^2 z}{\partial x^2} + \frac{\partial^2 z}{\partial y^2} = -\frac{p}{T} \quad \rightarrow \quad \nabla^2 z = -\frac{p}{T} \tag{7}$$

It is possible to obtain an approximate solution for the displacement that occurs in the direction of the applied pressure, defined by equation (7), using a numerical method.

Figure 22 illustrates an example of the results for the displacements using an approximate solution for 2D Poisson equation.

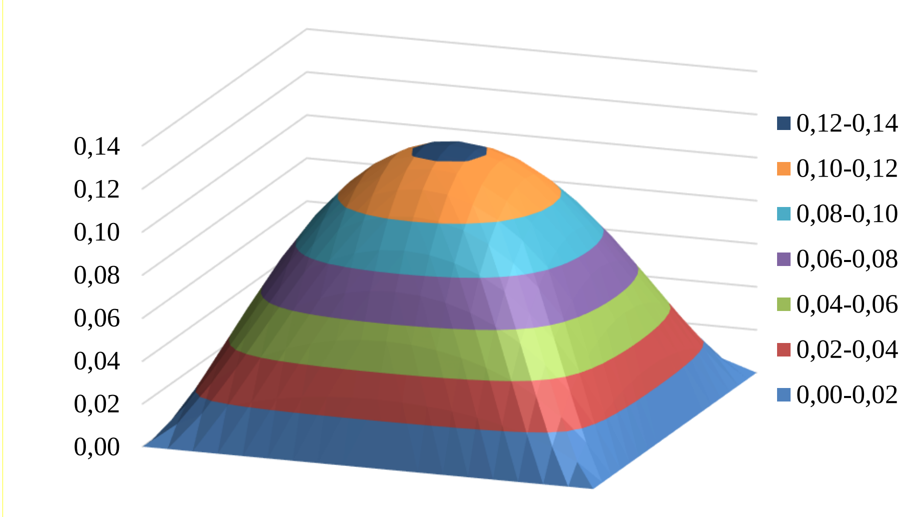

Figure 22 – Displacement determined through the numerical approach.

6. The GSC Approach

The experimental and the numerical investigations highlight the fact that the mesh mechanical behavior can be accurately described in terms of its mechanical properties. Furthermore, the achieved experimental and numerical results confirm that it is suitable to define the state of a gabion element with reference to different limits, such as service and ultimate conditions.

In this light, an analytical approach is then proposed to determine the out-of-plane behavior of a mesh subjected to an orthogonal pressure, as in the case of the outer face of a gabion within a retaining gabion structure. If a real structure is considered, the action on the outer face of the gabion can be assumed as a uniform pressure acting along its area of influence.

Considering the above structural conditions, a full mechanical characterization can be achieved either through tensile tests or through punching tests of the steel mesh. Both tensile and the punching test present a different way of characterizing the rupture condition of the material. Due to the different loading condition, also a different approach to interpret the overall behavior of the mesh is required.

The punching test can be then considered as an index test to define the not only the strength of the mesh depending on the applied force normal to the induced displacement, but also the whole mechanical behavior under different loading conditions. Furthermore, the analytical study of this mechanical condition shows that the overall punch behavior is led by the internal stress acting on the actual plane of the mesh.

When considering the hexagonal mesh of the gabion as an elastic membrane, the hypotheses established by the two-dimensional Poisson's equation are accepted and during the punching test it can be approximated to a circular isotropic membrane. The punching is performed by means of a cylindrical piston pressed against the membrane. In the analysis it is assumed that the piston is attached to the membrane. Therefore, the portion of the mesh under the piston can be eliminated from the membrane analysis. This approximation generates the domain shown in Figure 23, with two circumscribed circles. At the edge of the piston the displacement $w = w_0$, while at the edge of the membrane $w = 0$.

According to Santos Junior (2018) the maximum equivalent tensile strength (T) when the displacement is maximum ($w = w_0$) provided by the membrane along the edge of the piston (Figure 24) results to be:

$$F = 2\pi\, r_1 T \sin\alpha \qquad (8)$$

where F is the driving force of the punching test, r_1 is the radius of the punching element;

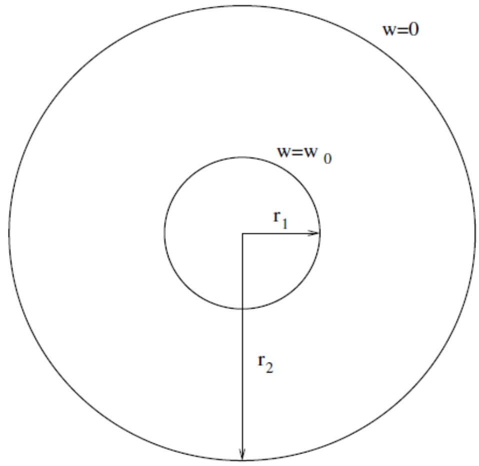

Figure 23 - Top view of the punching test approaching an isotropic elastic membrane.

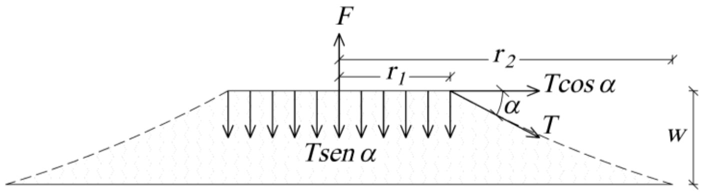

Figure 24 - Geometrical shape obtained during the punching test and rigid body diagram in a cross-section (SANTOS JUNIOR, 2018).

Plaut (2009) presents the solution of the ring membrane problem with the outer edge $r = r_2$ fixed and the inner edge $r = r_1$, with displacement w_0. The solution presented is based on Föppl-von Kármánn's theory. The displacement $w(r)$; $r_1 \leq r \leq r_2$ is given by:

$$w(r) = w_0 \frac{1-(r/r_2)^{2/3}}{1-(r_1/r_2)^{2/3}} \tag{9}$$

The inclination of the membrane at the piston edge is:

$$\tan\alpha = \frac{\partial w(r_1)}{\partial r} = \frac{2w_o}{3r_2\left[(r_1/r_2)^{2/3}-1\right](r_1/r_2)^{1/3}}$$

and $$\sin\alpha = \frac{\tan\alpha}{\sqrt{1+\tan^2\alpha}}$$

The deformation of the mesh in the direction r, for large displacements is given by (Timoshenko, 1959):

$$\varepsilon_r = \frac{\partial u}{\partial r} + \frac{1}{2}\left(\frac{\partial w}{\partial r}\right)^2 \tag{10}$$

where u is the radial displacement. Assuming that $\partial u / \partial r = 0$ near the edge of the piston, where the deformation ε_r is maximum:

$$\varepsilon_r(r) = \frac{1}{2}\left(\frac{\partial w(r)}{\partial r}\right)^2 \tag{11}$$

The tensile force depends on the normal displacement, w, and can be described by means of a new mechanical parameter: the Gabion Membrane Coefficient (GMC).

$$T(r) = \text{GMC}.\varepsilon_r(r) \tag{12}$$

According to equation 11 and deriving equation 9 with respect to r,

$$T(r) = \text{GMC}.\frac{2w_0^2}{9r_2^2\left[1-(r_1/r_2)^{2/3}\right]^2 (r/r_2)^{2/3}} \tag{13}$$

Substituting equation 13 into equation 8 and considering $r = r_1$,

$$\text{GMC} = F\left(\frac{9r_2^2\left[1-(r_1/r_2)^{2/3}\right]^2 (r_1/r_2)^{2/3}}{4\pi r_1 w_0^2 \sin\alpha}\right) \tag{14}$$

In this case, it is possible to relate the GMC to the force of the punching test of the mesh and the correspondent displacement w_o

$$F(r) = \text{GMC}\ \varepsilon_r(r) 2\pi\ r_1 \sin\alpha \tag{15}$$

The force versus displacement graph for each mesh type can be then plotted using the relevant GMC value in the equation (15). This also allows a comparison between experimental punch results and analytical solution, confirming the reliability of the proposed analytical approach. This comparison in the case of the 8x10, 2.7mm mesh is presented in Figure 25, where, Fp_{max} is maximum force and δp_{max} maximum displacement obtained from the punching test for the respective mesh.

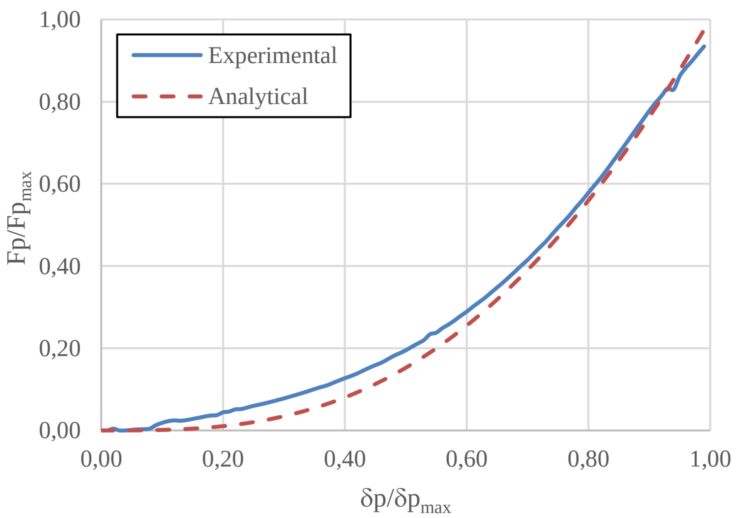

Figure 25 – Behavior of DT mesh under punch test, comparison of experimental results and GSC analytical approach.

6.1. The GSC Concept

The GMC is a mechanical parameter that translates the technical characteristics of the hexagonal mesh in terms of the mechanical properties of the steel wire. This parameter is directly derived from the punching test. Nevertheless, this new GMC parameter describes the initial mechanical behavior of both mesh and gabions. Nevertheless, the overview of the current normative requirements given in the introduction of this manual highlights as the mechanical behavior of the structure under design shall be verified considering the whole expected working life of the retaining wall. The variation of the mechanical performances over the time shall be then considered.

The most relevant degradation action to be considered among all is the corrosion process, since the mesh is exposed to the weather action. Passivating agents like steel alloy and plastic coatings are then provided against corrosion to increase the durability of these materials. Consequently, appropriate partial reduction factors should be considered in the proposed analytical approach. This allows to consider on one side the type of the environmental conditions and the conditions of exposure of the structure and on the other side the protective measures that are mainly depending on the provided coating.

The overall behavior of a gabion retaining structure under service conditions can be then investigated also considering its expected working life. From the analytical point of view, the GMC mechanical parameter suitable to describe the overall behavior of the mesh at t=0. Then, this shall be adequately reduced by a partial reduction factor f_{pr} that considers the above-mentioned degradation effects and the protective measures, namely the coating.

A new mechanical parameter is then created as Gabion Serviceability Coefficient (GSC) and its definition is shown in equation (16).

Finally, considering the displacement as the reference parameter to measure the stability of the structure, the retaining wall can be analyzed under serviceability conditions through this new GSC parameter.

$$\mathrm{GSC} = \frac{\mathrm{GMC}}{f_{pr}} \qquad (16)$$

where, f_{pr} is the partial reduction factor depending on the considered protective coating. A comprehensive description of the approach for the partial reduction factors is presented in APPENDIX A.

Two additional reduction factors are introduced to in addition to the previously mentioned one to verify the Service Limit States. These reduction factors consider both the variability of the filling properties of the gabion baskets and the mechanical properties of the mesh.

A first partial Reduction Factor ($f_{m,1}$) considers the variability of the filling properties of the gabion baskets. This variability is due to different causes such as different construction techniques, the skills of workers, the grading of the stones, the automatic or the manual filling of the baskets. All these aspects influence the void ratio and thus the mechanical performance of the basket. $f_{m,1}$ is assumed to be equal to 1.25.

A second partial Reduction Factor ($f_{m,2}$) considers the variability of the mechanical properties of the mesh. This variability is due to the intrinsic variation of the mechanical performances of the raw metallic wire constituting the baskets. This is directly reflecting on the mechanical performance of the mesh and thus of the GSC. $f_{m,2}$ is assumed to be equal to 1.15.

The product of both the above-mentioned Reduction Factors gives an overall Reduction Factor (f_m) directly applied to the GSC value. The f_m is equal to 1.44.

$$f_m = f_{m,1} \cdot f_{m,2} = 1.25 \cdot 1.15 = 1.44$$

The combination of these two factors results in a final f_m factor that shall be separately applied when the actual internal behavior of the mesh shall be computed. Equation (17) shows the final formulation including this reduction factor.

$$T(w) = \frac{\text{GSC}}{f_m}.\varepsilon(w) \quad (17)$$

Because of GSC, it is possible to calculate the deflection of the hexagonal mesh under the normal pressure acting on the front face of a retaining wall in long term condition. The GSC becomes then a new mechanical parameter suitable to define the required mesh performance. Furthermore, this results in a new methodology criterion to specify the gabions.

GSC represents a new analysis concept for designing gabion retaining walls. Hence, based on this new coefficient, it is possible to create a link between the mechanical behavior of the hexagonal mesh and the mechanical properties of the fill material obtained through the compression tests.

6.2. Internal stability

According to Santos Junior (2018) if the behavior of the gabion mesh under normal pressure respects the elastic membrane hypothesis, then it respects the 2D Poisson's equation (Figure 26). To determine the normal displacement on membrane, it is enough to introduce the normal pressure (p) on the membrane and the tensile force (T) which is a function of the deformation value of the elastic membrane and the appropriate value of GSC.

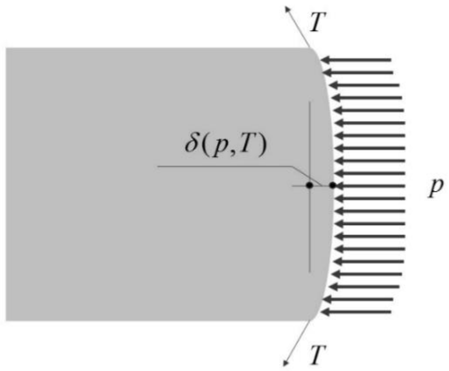

Figure 26 - Maximum Displacement due to the horizontal stress and the tensile strength.

Poisson's equation is a partial differential equation,

$$\nabla^2 \delta = f \qquad (18)$$

where ∇ is the Laplacian operator, and f and δ are real functions on a Euclidean space.

Considering the f equal to a unit value:

$$\nabla^2 \bar{\delta} = 1 \qquad (19)$$

and boundary condition according to Figure 27.

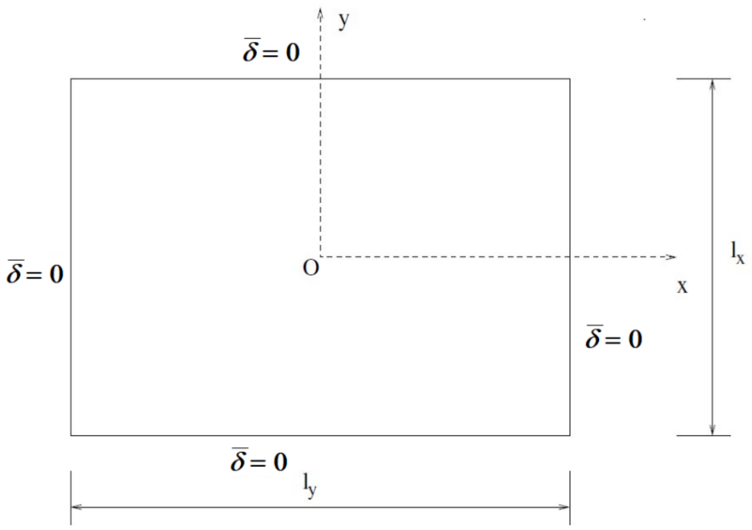

Figure 27 - Frontal view of the elastic membrane and boundary conditions.

and given the values of l_x and l_y it is possible to determine the horizontal displacement. Thus, one can compute:

$$\delta_d = \frac{p}{T}\bar{\delta} \qquad (20)$$

where δ_d is the maximum displacement in the direction of the working pressure; p is the uniform pressure and T is the tensile force of the mesh per unit length.

Considering that the deformed membrane has a parabolic shape its deformation is given by:

$$\varepsilon(\delta_d)=\left(\frac{\sqrt{l_x^2+16\delta_d^2}}{2l_x^2}+\frac{l_x^2\operatorname{arcsinh}\left(4\delta_d^2/l_x^2\right)}{8\delta_d^2}-1\right) \quad (21)$$

Thus,

$$T(\delta_d)=\frac{\text{GSC}}{f_m}.\varepsilon(\delta_d) \quad (22)$$

By means of a numerical method it is possible to calculate the value of the maximum horizontal displacement per unit for a $l_x = l_y = 1.0$m, $\overline{\delta}_{\max}$ = 0.073 and to the half-meter-high gabion l_x = 0.50m and l_y = 1.0m, $\overline{\delta}_{\max}$ = 0.027.

Then, through the value of the uniform pressure acting on the hexagonal mesh panel and the tensile strength obtained by the displacement, it is possible to determine the value of the maximum deflection that the hexagonal mesh of the gabion can be submitted in strata of 1.00 m or 0.50 m gabion.

The gabion retaining walls are composed by layers and each gabion layer has a height of one meter or half a meter. Each gabion layer is subjected to a uniform vertical pressure due to action of the upper layers and the retained material. The horizontal pressure can be computed through equation 6 and, therefore the maximum horizontal mesh displacement is obtained from the graph of Figure 28.

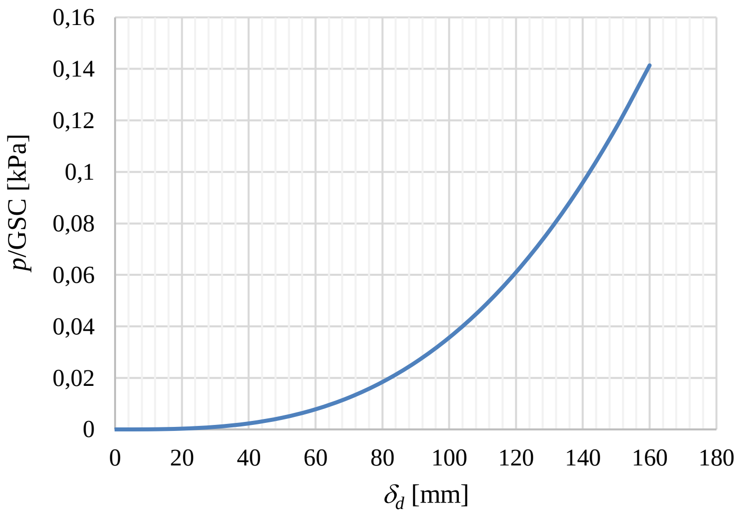

Figure 28 - Maximum horizontal displacement determined by horizontal pressure and the GSC value for l_x = 1.0m.

The internal stability criterion is then calculated as the ratio between the reference displacement value, and the actual horizontal displacement (bulging) computed per each layer. As a common approach, the overall allowable reference displacement value for a gabion retaining structure is usually considered as a percentage of the wall height "*H*". Some reference examples, showing the displacement of the whole wall, are presented hereafter.

Table 4. Example of reference values of horizontal displacement.

	Reference displacement	Additional notes	Reference
Permissible	From 1% to 1.5% H	H from 6m to 8m, δ =6cm H from 6m to 8m, δ =13.5cm	Bathurst et al. 1995
	From 1% to 2% H	H=6m, δ from 6cm to 12cm	EBGEO, 2010
	1.5% H	$H \leq 3.3$m, $\delta \leq 4.95$cm	Pianc, 2001
	2.0% H	H=6m, δ =12cm	Huang et al. 2009
	250·Kh,max	0.2g, δ =5cm 0.4g, δ =10cm	AASHTO, 2002
	300·Kh,max	0.2g, δ =6cm 0.4g, δ =12cm	CEC, 1994
Limiting	5% H	H=3m, δ =15cm H=6m, δ =30cm	Koseki et al. 1998 Huang et al. 2009

In the case of a gabion retaining wall the reference value to evaluate the internal stability can be then considered following the same approach. In this light, the reference value is then depended both on the geometry of the wall and on the considered gabion typology. These aspects are then considered referring to the overall height of the structure *"H"* and to the height of the single gabion height *"l"* respectively (Figure 29). Indeed, two possible gabion heights can be considered, namely 1.0 m and 0.50 m. The strength and the displacement of the latter are increased and reduced respectively referring to the former, as confirmed both by the experimental tests and the numerical analyses.

Based on the above approach, the reference values displacement to be considered for the computation of the final safety factors (FoS) are then computed as follows:

- Reference displacement:

$$\delta_{ref} = \frac{l}{10}\left(1 + \frac{H}{15}\right) \tag{21}$$

where, *l* is the layer height and *H* is the wall height.

- Reference safety factor (FoS):

$$FoS = \frac{\delta_{ref}}{\delta_d} \tag{22}$$

where, δ_d is the maximum horizontal displacement per layer.

- The minimum admissible safety factor (FoS) in a long-term design condition shall be considered equal to 1.40.

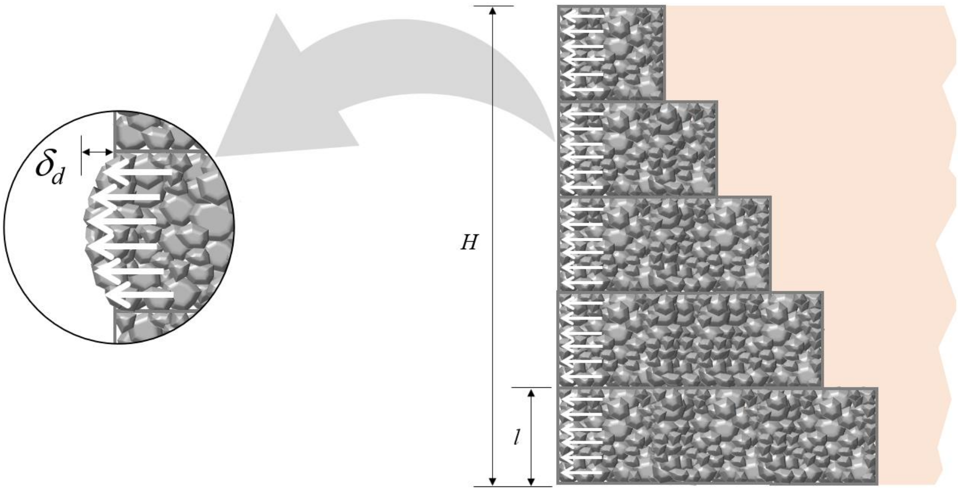

Figure 29 - Maximum horizontal displacement per layer in function of height.

The final Factor of Safety (*FoS*) to evaluate the internal stability can be then computed as the ratio between the reference value of displacement δ_{ref} and the actual value of displacement δ_d under service conditions. The latter value is computed through the GSC coefficient and based on the proposed approach in section 6.2. As presented on the previous sections, this also allows the long-term effects to be considered in this serviceability analysis.

7. Worked example

For the purpose of exemplification will be made the analysis of the load capacity of a retaining wall in gabion with height 8.0 m (Figure 32), using Gabion PoliMac™ 80/489.

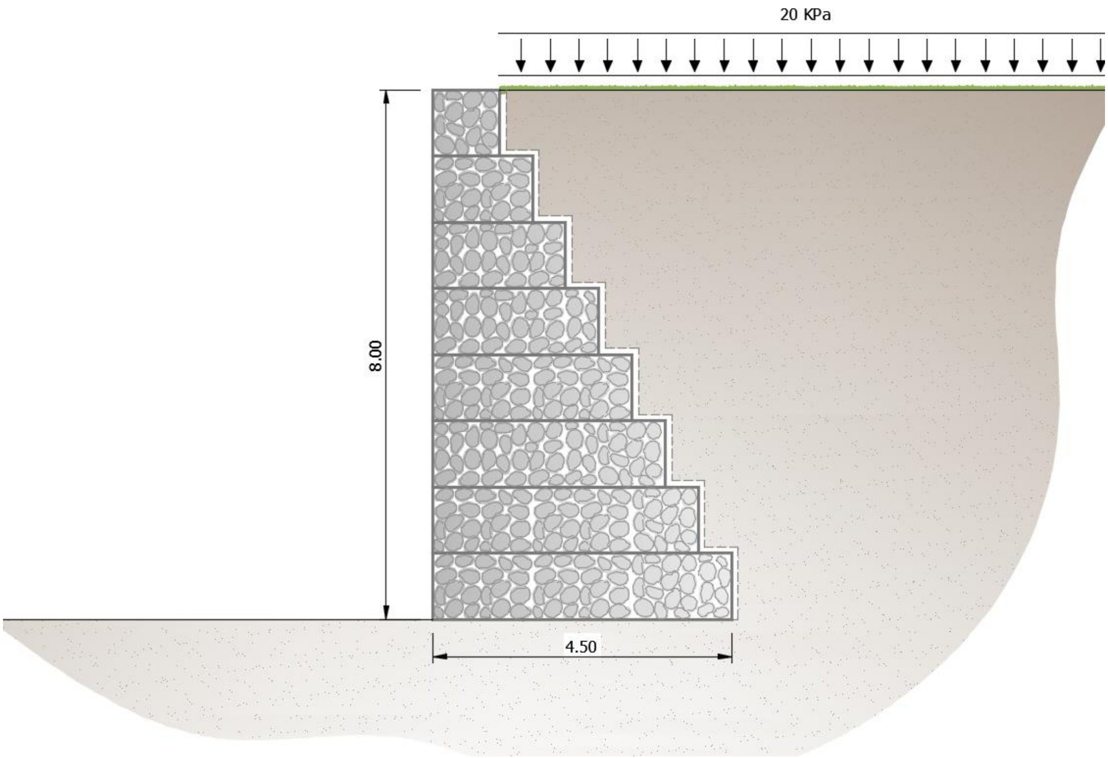

Figure 32 – Gabion wall with 8.00 m of height, composed of gabion box of 1,00 m.

Fill material	Foundation
Specific weight = 18 kN/m³	Specific weight | 19 kN/m³
Internal friction angle = 30 degrees	Internal friction angle | 32 degrees
Applied loads:	Cohesion | 10KPa
On the fill, q_1 = 20 kN/m²	Bering capacity | 350 KPa
	Angle between the gabions and the backfill | δ=28.5 (5% of reduction)

a) Internal Stability

The pressure applied on each layer of gabion wall can be calculated by the equation 34:

$$\sigma_{máx} = \frac{N}{2d} \qquad (34)$$

For the external stability analysis to find the forces and the moments, the GawacWin® software (Gabions Wall Calculation for Windows) is used to provide the results of the vertical pressure on each layer along a gabion wall (Table 7).

Table 7 - Results of vertical pressure on each gabion layer.

Layer	Height (m)	σ_{max} (kPa)
1	1.00	21.60
2	2.00	54.02
3	3.00	88.63
4	4.00	123.34
5	5.00	157.60
6	6.00	191.33
7	7.00	224.59

From the equation 6, it is possible to obtain the horizontal pressure and using the approach presented in section 6, it has the FoS by layer. (Table 8).

Table 8 – Vertical and Horizontal pressures and resulting final FoS.

Layer	Vertical pressure (kPa)	Horizontal pressure, *p* (kPa)	FoS
1	21.60	2.16	2.73
2	54.02	5.40	2.01
3	88.63	8.86	1.70
4	123.34	12.33	1.52
5	157.60	15.76	1.40
6	191.33	19.13	1.31
7	224.59	22.46	1.24

Layers 6 and 7 showed FoS values lower than allowed (FoS ≥ 1,40). As a solution, gabions with a height of 0.50 m (Figure 36) should be proposed, replacing layers 6 and 7 and recalculating the FoS. The results are shown in Table 9.

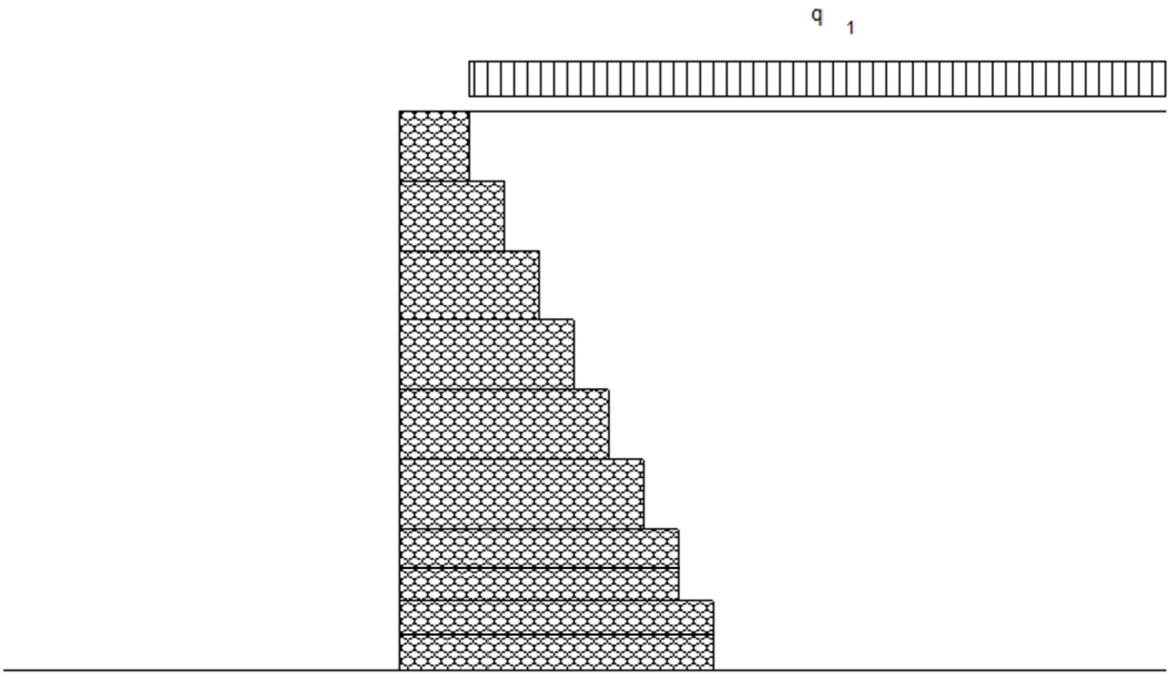

Figure 36 – Gabion wall with 8.00 m of height, composed of gabion box of 0,50 m and 1,00 m.

Table 9 – Vertical and Horizontal pressures and resulting final FoS.

Layer	Vertical pressure (kPa)	Horizontal pressure, *p* (kPa)	FoS
1	21.60	2.16	2.73
2	54.02	5.40	2.01
3	88.63	8.86	1.70
4	123.34	12.33	1.52
5	157.60	15.76	1.40
6	191.33	19.13	1.83
7	189.72	18.97	1.84
8	224.59	22.46	1.74
9	221.40	22.14	1.75

In the case of half-meter gabions, the GSC's value is double that of the one-meter-high gabion. This demonstrates that by appropriately using the GSC concept it is possible to reduce the deformations acting on the gabion during project definition.

References

AASHTO Standard specifications for highway bridges [Book]. - Washington, D.C. : American Association of State Highway and Transportation Officials, 2002. - Vol. Secs. 3 and 7.

ASSOCIAÇÃO BRASILEIRA DE NORMAS TÉCNICAS – ABNT NBR 12767: Rochas para revestimento - determinação da resistência à compressão uniaxial: método de ensaio. Rio de Janeiro: ABNT, 1992.

ASSOCIAÇÃO BRASILEIRA DE NORMAS TÉCNICAS - ABNT NBR 8964: Arames de aço de baixo teor de carbono, revestidos, para gabiões e demais produtos fabricados com malha de dupla torção, Rio de Janeiro, 2013.

ASSOCIAÇÃO BRASILEIRA DE NORMAS TÉCNICAS - ABNT NBR 6207: Arame de aço - Ensaio de tração, Rio de Janeiro, 1982.

ASSOCIAÇÃO BRASILEIRA DE NORMAS TÉCNICAS - ABNT NBR 10514: Redes de aço com malha hexagonal de dupla torção, para confecção de gabiões – Especificação, Rio de Janeiro, 1988.

ASSOCIAÇÃO BRASILEIRA DE NORMAS TÉCNICAS - ABNT NBR 6122: Projeto e execução de fundações, 2010

ASTM INTERNATIONAL - A 975: Standard Specification for Double-Twisted Hexagonal Mesh Gabions and Revet Mattresses, 2011.

BRITISH STANDARDS INSTITUTION – BS 8006-1: Code of practice for strengthened / reinforced soils and other fills, 2016.

BRITISH STANDARDS INSTITUTION - BS EN 10223-3: Steel wire and wire products for fencing and netting. Hexagonal steel wire mesh products for civil engineering purposes, 2013.

NORMA BOLIVIANA - NB 709: Alambre de acero de bajo contenido de carbono, revestido, para gaviones y otros productos fabricados con malla hexagonal de doble torsión – Especificaciones (Tercera revisión), 2014.

NORMA BOLIVIANA - NB 710: Redes de acero con malla hexagonal de doble torsión para fabricación de gaviones - Especificaciones (Primera revisión), 2000.

NORMA BOLIVIANA - NB 1224001: Especificaciones para gaviones tipo caja y tipo colchón, producidos con malla hexagonal de doble torsión y fabricados con alambre que cumplen con la norma NB 709 (Correspondiente a la norma ASTM A 975:1997), 2003.

AGOSTINI, R.; CESARIO, L.; CONTE, A.; MASETTI, M.; AND PAPETTI, A. Flexible gabion structures in earth retaining works, Officine Maccaferri S.p.A., Bologna, Italy, 1987.

BATHURST, R.J., SIMAC, M.R. AND SANDRI, D., Lessons learned from the construction performance of a 14 m high segmental retaining wall. Proc. Geosynthetics: Lessons, 1995.

DELL'AVANZI, E; H. GODOY, G.P; BERNARDES, e H. JARROUGE. Estudo do comportamento de estruturas grampeadas utilizando modelos reduzidos - conceitos teóricos para garantia da similitude modeloprotótipo. 6 f. In: XIII Congresso Brasileiro de Mecânica dos Solos e Engenharia Geotécnica, Curitiba, 2006.

EBGEO, Deutsche Gesellschaft für Geotechnik, Empfehlungen für den Entwurf und die Berechnung von Erdkörpern mit Bewehrungen aus Geokunststoffen- EBGEO, Ernst & Sohn, Berlin, 2010.

EBGEO, Deutsche Gesellschaft fur Geotechnik, EBGEO: Recommendations for design and analysis of earth structures using geosynthetic reinforcements. 3rd ed. Munich: Ernst and Sohn, 2011.

GOMES, Joaquim Francisco da Silva. Mecânica dos Materiais e Estruturas Lineares. Teoria e Aplicações, Capítulo V - Torção de Peças Lineares. Porto, FEUP - Publicação Didática. 2009.

HUANG C. C., WU S. H. and WU H. J. Seismic Displacement Criterion for Soil Retaining Walls Based on Soil Strength Mobilization [Journal] // J. Geotech. Geoenviron. Eng.. - [s.l.] : ASCE, 2009. - 135. - pp. 74-83, 2009.

KOSEKI, J., TATSUOKA, F., MUNAF, Y., TATEYAMA, M. AND KOJIMA, K., A modified procedure to evaluate active earth pressure at high seismic loads, Soils and Foundations, Spe-cial Issue on Geotechnical Aspects of the January 17 1995 Hyogoken-Nambu Earthquake, 2, 209-216, 1998.

PIANC, Seismic Design Guidelines for Port Structures, Working Group n.34 of the Maritime Navigation Commission, International Navigation Association, Balkema, Lisse, 474 pp, 2001.

PLAUT, R.H., Linearly elastic annular and circular membranes under radial, transverse, and torsional loading. Part I: large unwrinkled axisymmetric deformations. Acta Mechanica 202 (1–4), 79–99, 2009.

SANTOS JUNIOR, Petrucio José, Gabiões e estruturas de arrimo: análise teórico-numérico-experimental do comportamento mecânico - Campinas, SP: [s.n.], Tese de Doutorado - Universidade Estadual de Campinas, Faculdade de Engenharia Civil, Arquitetura e Urbanismo. 2018.

ŠMILAUER, V., CATALANO, E., CHAREYRE, B., DOROFEENKO, S., DURIEZ, J., GLADKY, A., KOZICKI, J., MODENESE, C., SCHOLTÈS, L., SIBILLE, L., STRÁNSKÝ, J., THOENI, K. Yade Documentation. The Yade Project. (http://yade-dem.org/doc/), 2010.

THOENI, Klaus; LAMBERT, Cèdric; GIACOMINI, Anna; SLOAN, Scott W. Discrete Modelling of a Rockfall protective system, II International Conference on Particle-based Methods-Fundamentals and Applications, PARTICLES 2011, Barcelona, Spain. 2011.

TIMOSHENKO, S. P., Theory of Plates and Shells. New York McGraw-Hill, pp. 396-428, 1959.

Appendix A - Determination of the Reduction Factors to compute GSC (Gabion Serviceability Coefficient) in gabion structures

This note provides a technical explanation of reduction factors to be used in design of gabion wall structures. Factors include the effects of degradation typical of metal coatings and polymer coatings.

Long term durability of wires

Main factors affecting durability of steel wire meshes exposed in outdoor or in soil embedment are:

1. Corrosion, (metal coatings) and environmental effects;
2. Installation damage, both for metal and polymer coatings, during filling and material handling operations;
3. UV ray's exposure, for polymer coatings, causing loss of elongation and mechanical strength.
4. Abrasion, both for metal and polymer coatings, due to wearing effects of sediments in hydraulic structures or in soils.
5. Temperature variations & pH effects, for polymer coatings, due to the contact in water in hydraulic structures or soils;

As far as points 1 and 2 above, international standards (ISO9227 and ASTM D5818) allow to determine reduction factors based on evaluation of either loss of mechanical property (elongation, tensile strength) or loss of coating integrity.

As for point 3, the variation of mechanical property after UV ray's exposure (ISO 4892-3) can also be extra-polated in a reduction factor, obtained by correlating residual tensile strengths of PVC and PoliMac™ after 2500 hours UV exposure.

As for abrasion, pH effects, and temperature variations, currently there are no standards to provide an interpretation with a reduction factor, in terms of coating life.

In order to account for their effects, as well as manufacturing and extrapolation of data, an overall coefficient of indetermination of 0.9 is assumed, on the safe side for the PoliMac™ coating.

Corrosion and environmental effects

Corrosion and environmental effects are regarded as the most critical aspects affecting durability of wires in outdoor environments. Several studies express the resistance against corrosion for metallic coatings as loss of coating mass per unit area (g/m²).

The most common test against corrosion for metallic coatings is salt spray. The test procedure is described in ISO 9227. The test consists in exposing samples in a highly concentrated salt spray environment for a number of hours, observing when Dark Brown Rust appears on the surface. PoliMac^{TM} and PVC coated wire mesh samples were exposed up to 6000 hours without appearance of Rust (Figure A.1).

Equally from tests evidence shows that exposed samples of zinc coated, GalMac (Zn95Al5), GalMac4R (Zn90Al10), all in Class A, reach an average time before rust appearance of 500, 1500, and 3000 hours. Conservatively for Polymer coated steel wire mesh the limit number is set to 6000 hours, even if actually no rust was visible. Metallic coatings are referred as a percentage referred to that value.

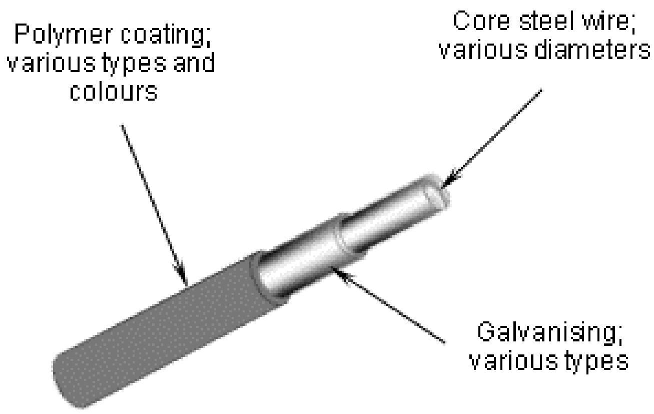

Figure A.1 - Wire types used for steel wire mesh products.

Installation Damage

Installation damage is related to the potential damage of the organic, or of the metallic protection caused during filling or handling of the baskets. The procedure, which is standard practice for soil reinforcement products, is described in ASTM D5818. For the gabion filling, results obtained by this test using coarse aggregates (gravel) quantify the abrasion effect produced by the rocks during the filling of the basket, on the safe side (Table A.1). Figure A.1 shows a linear regression curve based on the points in Table A.1.

Table A.1 – Abrasion effect produced by the rocks according to ASTM D5818.

	UTS min [kN/m]	n/16	RFid
No wire cuts	50.0	0.00	1.000
1 wire cut	47.8	6.25	1.046
2 wires cuts	43.4	12.5	1.152
3 wires cuts	40.9	18.75	1.222

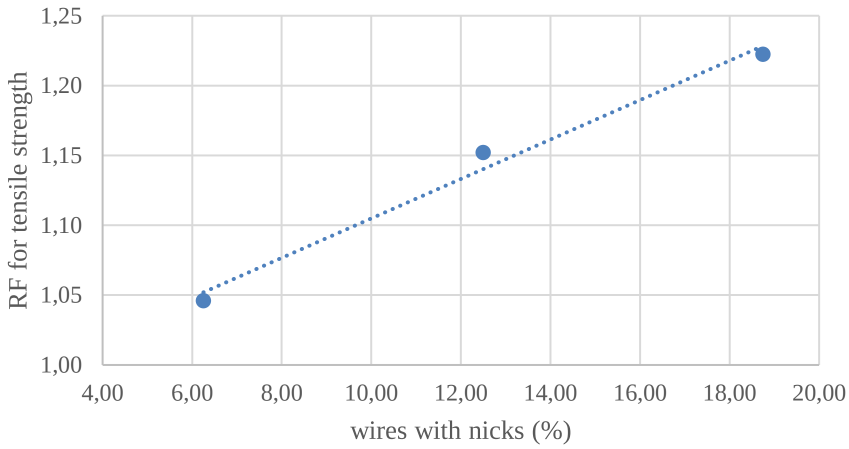

Figure A.1 – Linear regression curve based of wires with nicks.

The procedure in ASTM D5818 evaluates per each specimen of wire mesh the percentage of visible nicks per area. Technical Note "TN-DT-021A_Partial factors of Terramesh_Rev4" describes how to correlate this value with the reduction of mesh strength.

Installation damage tests were conducted at TRI Texas (USA) for PoliMac™ and for PVC coated wire mesh. For PoliMac™ coated steel wire mesh embedded in coarse aggregates (20-40mm) installation damage tests provided 8.7% of the tested area with wire nicks. For PVC coated wire mesh, test in coarse gravel (20-40mm) provided 12.5% wire nicks. Graph in fig. 1 shows the correlation between the drop-in strength of the steel mesh and the percentage wire nicks per area obtained from the test.

The trendline of strength reduction with 1, 2 and 3 initial wire cuts allow to calculate the reduction factor as a function of the wire nicks. We can see that at 8.7% the graph provides a value of RF= 1.087, resulting in a Damage Factor of 1/1.087 = 0.920. For the PVC the value of 12.5% corresponds to a value of RF=1.15, resulting in a damage factor of 1/1.15 = 0.870. Conservatively for polymer coated steel wire mesh, the metallic coated mesh is not assumed to suffer any damage due to installation. The Table A.2 reports final RF factors at 120 years, as the product of Corrosion and Damage Factors.

Table A.2 – Reduction factors of the gabion mesh at 120 years.

	Corrosion & Environmental effects	Installation damage	UV degradation	Indetermination & Man./extrap. of data	RF 120yrs
PoliMac™	0.952	0.920	1.00	0.90	0.788
PVC	0.952	0.870	0.74	0.90	0.551
GalMac 4R (Class A)	0.500	1.000	1.00	0.90	0.450
GalMac (Class A)	0.250	1.000	1.00	0.90	0.225
Zinc (Class A)	0.083	1.000	1.00	0.90	0.075

Appendix B – Gabion International Standards

ASTM A975-11 Standard Specification for double-Twisted Hexagonal Mesh Gabions and Revet Mattresses;

BS EN 10223-3:2013 Steel wire and wire products for fencing and netting. Hexagonal steel wire mesh products for civil engineering purposes;

AUS_R55 - Rock filled gabions and mattresses;

BS 8002 2015 - Code of practice for earth retaining structures;

FRA_NF P94-325-1 Execution of special geotechnical works - Gabion works;

FRA_NF P94-325-2 Execution of special geotechnical works - Gabions in wire mesh with hexagonal double twist;

INDIA_IS-16014-2012-2_GABIONS;

RUS_ Gabion manufactured with double twisted hexagonal wire mesh;

SANS – 1580 – 2010 – Hexagonal steel wire mesh gabions and revet mattresses;

SPA_UNE_36730 2006 - Gabions mesh lattice hexagonal mesh galvanized, or galvanized steel wire and PVC coated;

UNI 11437:2012 Rockfall Protective Measures – Tests on Meshes for Slopes Coverage;

YB T4221-2016 – Steel wire for machine woven steel wire mesh with engineering;

ISO 9224:2012 Corrosion of metals and alloys – Corrosivity of atmospheres – Guiding values for the corrosivity categories;

NMX-B-085-CANACERO-2005 - Standard Specifications for Steel Mesh Products shaped in Triple Twist galvanized or coated additional Polyvinyl Chloride (PVC);

NB 709-2014 Coated, low carbon steel wire for gabions and other products manufactured with double-twisted hexagonal mesh - Specifications (Third revision);

NB 710- 2000 Steel networks with hexagonal double torsion mesh for gabion manufacture - Specifications (First revision);

NB 1224001: 2003 Specifications for box type and mattress type gabions, produced with double twisted hexagonal mesh and manufactured with wire that comply with the NB 709 standard (Corresponding to ASTM A 975: 1997);

NorGeoSpec 2002 – A Nordic System for specification and control of geotextiles in roads and other trafficked areas;

PNS 113-2005 – Specification for low carbon steel wires – Plain/annealed/zinc-coated;

RSTA Code of Practice for Geosynthetics and Steel Meshes.